Received: 17 February 2025 | Revised: 28 July 2025 | Accepted: 29 July 2025

DOI: 10.1111/bph.70180

RESEARCH ARTICLE

Angiotensin II-induced phosphorylation of CHK1 at serine-280 drives cardiac remodelling by direct phosphorylation of JAK1, thus activating JAK1-STAT signalling in murine cardiomyocytes

Zheng Xu[1,2] | Yihan Shen[2] | Xiaoting Luo[3] | Jingru Wang[2] | Qian Zhou[2] | Xue Han[2] | Juan Ren[2] | Lihong Wang[1] | Guang Liang[1,2]

[1]Heart Center, Department of Cardiovascular Medicine, Zhejiang Provincial People's Hospital, Affiliated People's Hospital, Hangzhou Medical College, Hangzhou, China

[2]School of Pharmaceutical Sciences, Hangzhou Medical College, Hangzhou, China

[3]Department of Nursing, Urology and Nephrology Center, Department of Urology, Zhejiang Provincial People's Hospital, Affiliated People's Hospital, Hangzhou Medical College, Hangzhou, China

Correspondence
Prof. Guang Liang, Hangzhou Medical College, Hangzhou 310014, Zhejiang, China.
Email: wzmcliangguang@163.com

Funding information
National Natural Science Foundation of China, Grant/Award Number: 82300532; Natural Science Foundation of Zhejiang Province, Grant/Award Number: LQ22H020002; Medical and Health Research Project of Zhejiang Province, Grant/Award Number: 2025KY023; Fundamental Research Funds for the Hangzhou Medical College, Grant/Award Number: KYZD2023004

Background and Purpose: Cardiac remodelling is a common pathological process of heart disease. Checkpoint kinase 1 (CHK1), a key regulator of the DNA damage response and cell cycle, is well-studied in oncology, but its role in pathological cardiac remodelling remains unclear. Here, we investigated the activation of CHK1 and its effects in mouse models of cardiac remodelling induced by angiotensin II.

Experimental Approach: We used co-immunoprecipitation and mass spectrometry (Co-IP/MS) to identify the substrate kinase of CHK1. Cardiac remodelling in C57BL/6 mice and hypertrophy in primary neonatal rat cardiomyocytes (NRCMs) was induced with angiotensin II. These models were treated with the CHK1 selective inhibitor CCT245737 or the JAK1 inhibitor upadacitinib.

Key Results: In vitro and in vivo, angiotensin II selectively activated phosphorylation of CHK1 at serine-280 (S280), but not at S345, in cardiomyocytes, without altering levels of CHK1 protein. Inhibition of CHK1 with CCT245737 suppressed angiotensin II-induced hypertrophy in NRCMs. Such hypertrophy was enhanced by the phosphomimetic CHK1 S280E mutant but was attenuated by the inactivating CHK1 S280A mutant. Co-IP/MS revealed that, in cardiomyocytes, JAK1 is the substrate protein of CHK1. Angiotensin II promoted CHK1 interaction with JAK1 to induce JAK1 phosphorylation and activation of JAK1-STAT3 signalling. In mice, both CCT245737 and upadacitinib reversed angiotensin II-induced cardiac remodelling and dysfunction.

Conclusions and Implications: Cardiomyocyte CHK1 S280 phosphorylation is a key step in angiotensin II-induced cardiac remodelling, through activation of the JAK1-STAT3 pathway. Pharmacological inhibition of CHK1 could be a potential therapeutic strategy for hypertensive heart failure.

KEYWORDS
angiotensin II, cardiac remodelling, checkpoint kinase 1, JAK1, STAT3

Abbreviations: Ang II, angiotensin II; ANP, atrial natriuretic peptide; β-MyHC, β-myosin heavy chain; BNP, brain natriuretic peptide; CCT, CCT245737; CHK1, checkpoint kinase 1; DAPI, 4′,6-diamidino-2-phenylindole; DDR, DNA damage response; H&E, haematoxylin–eosin; JAK1, Janus kinase 1; NRCMs, neonatal rat cardiomyocytes; UPA, upadacitinib.

Zheng Xu and Yihan Shen contributed equally to this work.

1 | INTRODUCTION

Cardiac hypertrophy and remodelling are characteristic features of several cardiovascular diseases, including hypertension, heart failure and myocardial infarction (Frantz et al., 2022; Martin et al., 2023). A key molecular mediator of these pathological changes is **angiotensin II** (Ang II), a critical effector agent of the renin–angiotensin system, known to induce cardiomyocyte hypertrophy, fibrosis, and ultimately heart failure through its engagement with various downstream signalling pathways (Forrester et al., 2018; Frangogiannis, 2021). While the signalling events triggered by Ang II have been widely studied, the exact molecular mechanisms underlying Ang II-induced cardiac remodelling remain incompletely understood.

Checkpoint kinase 1 (CHK1) is a serine/threonine protein kinase traditionally recognised for its role in the DNA damage response (DDR), where it preserves genomic integrity by initiating DNA repair mechanisms and cell cycle checkpoints (Dai & Grant, 2010; Patil et al., 2013). Based on this property, targeting of the CHK1 pathway to contribute to effective cancer treatment has been well-researched and validated (Dai & Grant, 2010; Osborne et al., 2016), leading to the development of small-molecule CHK1 inhibitors, some of which have advanced into clinical trials (Dai & Grant, 2010; Jiang et al., 2024; Osborne et al., 2016). As a protein kinase, CHK1 contains multiple phosphorylation sites, among which the phosphorylation of CHK1 at serine 345 (S345) has long been established as a marker of CHK1 activation in response to genotoxic stress (Dai & Grant, 2010). Recent evidence suggests that other phosphorylation sites on CHK1, such as serine 280 (S280), also play critical roles in modulating the kinase's activity in different contexts (Borenas et al., 2024; Nguyen et al., 2023; Yuan et al., 2014). Interestingly, recent studies suggest that the function of CHK1 extends beyond the oncology realm, playing roles in kidney injury (Ajay et al., 2014), myocardial infarction (Fan et al., 2020; Wei et al., 2024), inflammation and cellular senescence (Gioia et al., 2023). In particular, Wang's team showed that myocardial overexpression of CHK1 promoted cardiomyocyte proliferation and improved cardiac function in models of myocardial infarction and ischaemia–reperfusion injury (Fan et al., 2020; Wei et al., 2024). Moreover, a recent study further showed that CHK1 alleviates ischaemia–reperfusion injury and restores mitochondrial dynamics in cardiomyocytes through a **SIRT1**-dependent mechanism (Yang et al., 2025). Despite these advances, the role of CHK1 in cardiovascular disease, particularly in the context of Ang II-induced cardiac injury, has been minimally investigated. Considering that the CHK1 inhibitors have been studied in anti-cancer clinical trials, demonstrating the role and regulating mechanism of CHK1 in the heart may provide new clinical applications for these inhibitors.

In this study, we aimed to elucidate the role of CHK1 in Ang II-induced cardiac remodelling. We found that CHK1 S280 phosphorylation serves as a critical regulatory node in Ang II-challenged cardiomyocytes, driving the downstream activation of **JAK1** and **STAT3**, thereby mediating pathological hypertrophy and cardiac dysfunction. This study provides new insights into the molecular mechanisms of cardiac hypertrophy and highlights CHK1 as a potential therapeutic target for the treatment of heart failure.

What is already known?

- CHK1 is a serine/threonine kinase essential for DNA damage response and cell cycle regulation.
- Phosphorylation of CHK1 at Serine-345 (S345) is critical for the activation and function of CHK1.

What does this study add?

- Angiotensin II selectively induces CHK1 S280 phosphorylation in cardiomyocytes, promoting CHK1 interaction with JAK1.
- Inhibition of CHK1 S280 phosphorylation suppressed JAK1-STAT3 activation and normalised angiotensin II-induced cardiac remodelling.

What is the clinical significance?

- Our findings reveal a non-canonical role of CHK1 in angiotensin II-induced pathological cardiac remodelling.
- Targeting CHK1 S280 phosphorylation offers a promising therapeutic strategy for hypertensive heart failure remodelling.

2 | METHODS

2.1 | GEO data analysis

We analysed publicly available gene expression datasets to assess CHK1 transcription levels. Specifically, we examined data from GSE19210 (Brooks et al., 2010) and GSE1621 (Zhao et al., 2004), which are available in the Gene Expression Omnibus (GEO) to assess CHK1 transcription levels. Additionally, we analysed single-cell RNA-seq data from GSE193346 (Feng et al., 2022) to confirm the expression distribution of CHK1 in heart cells.

2.2 | Animal experiments

All animal care and experimental procedures were approved by the Institutional Animal Care and Use Committee of Zhejiang Center of Laboratory Animals, Hangzhou Medical College (Approval Number: ZJCLA-IACUC-20010926). Animal studies are reported in compliance with the ARRIVE guidelines (Percie du Sert et al., 2020) and with the recommendations made by the *British Journal of Pharmacology* (Lilley et al., 2020).

Ten-week-old male C57BL/6J mice (weight: 22–24 g) were obtained from the Zhejiang Center of Laboratory Animals. The mice were housed in specific pathogen-free (SPF) cages (≤5 mice per cage) under standard environmental conditions (23 ± 2°C, 12-h light/dark cycle, humidity of 55–65%) with ad libitum access to food and water at the Zhejiang Center of Laboratory Animals, Hangzhou Medical College (Licence number: SYXK[Zhe] 2019–0011). Studies were designed to generate experimental groups of equal size using randomisation and blinded analysis.

2.2.1 | Experimental procedures

a. To investigate CHK1 phosphorylation in vivo, mice received chronic Ang II infusion via osmotic minipumps (model 1,004, ALZET), delivering Ang II subcutaneously at a rate of 1000 ng kg^{-1} min^{-1} for up to 7 days. Mice were randomly divided into four groups based on the duration of infusion: 0, 3, 5, and 7 days. Each group consisted of five mice. At the designated time points, mice were overdosed with pentobarbital sodium, and heart tissues were harvested for further analysis.
b. To better evaluate the progression and effectiveness of Ang II-induced cardiac remodelling, mice were infused with Ang II at the same rate (1000 ng kg^{-1} min^{-1}) for up to 4 weeks, with weekly echocardiographic monitoring. Mice were randomly divided into five groups according to the infusion duration: 0, 1, 2, 3, and 4 weeks. Each group consisted of six mice. At each indicated time point, mice were overdosed with pentobarbital sodium, and heart tissues were harvested for further analysis.
c. To assess the impact of CHK1 and JAK1 inhibition on Ang II-induced cardiac remodelling, mice were treated with CHK1 inhibitor **CCT245737** (CCT; 1 mg kg^{-1}) or JAK1 inhibitor **upadacitinib** (UPA, 5 mg kg^{-1}), administered orally every other day for 2 weeks. Cardiac remodelling was induced via subcutaneous Ang II infusion at the rate of 1000 ng kg min^{-1} for 4 weeks, with a control group receiving saline-filled minipumps. Blood pressure was monitored weekly from baseline (week −1) to week 4 using a telemetric blood pressure system (BP-2010A, Softron Biotechnology), as previously described (Xu et al., 2022). Cardiac function was determined by echocardiography. The mice were divided into four groups: (1) Saline, (2) Ang II, (3) Ang II + CCT (1 mg kg^{-1}), and (4) Ang II + **UPA** (5 mg kg^{-1}). Both inhibitors were dissolved in a vehicle consisting of 5% DMSO, 30% PEG 300, 5% Tween 80 and 60% distilled water. Vehicle-only treatments were given to the saline and Ang II groups. At week 4, following echocardiography, mice were humanely killed (overdose of pentobarbital sodium), and blood and heart tissues were collected for further analysis.

2.2.2 | Immunoblotting and Co-IP

Total protein from heart tissues and cultured cells were extracted using radioimmunoprecipitation assay buffer (RIPA) lysis buffer supplemented with a mixture of protease and phosphatase inhibitors. Protein concentration was determined using the bicinchoninic acid (BCA) Protein Assay Kit. Proteins were separated by sodium dodecyl sulphate polyacrylamide gel electrophoresis (SDS-PAGE) and then transferred to polyvinylidene fluoride (PVDF) membranes. Thereafter, the PVDF membranes were blocked with a commercial blocking buffer and incubated with the corresponding primary antibody overnight at 4°C, followed by appropriate secondary antibodies. Protein bands were visualised with enhanced chemiluminescence reagent and viewed using FUSION-FX6.EDGE imaging system (Vilber, Collégien, France). Co-IP was performed using the Protein A/G Magnetic beads kit (Yeasen, Shanghai, China) according to the manufacturer's instructions. The goat-purified IgG was used as a negative control for Co-IP. All immunoassay procedures used comply with the recommendations made by the *British Journal of Pharmacology* (Alexander et al., 2018).

2.3 | Quantitative polymerase chain reaction (PCR) assay

Total RNA from heart tissues and cells was isolated and purified using standard techniques. Primers based on the mRNA sequences designed from the National Center for Biotechnology Information (NCBI) database were synthesised and obtained from Generay Biotech (Shanghai, China). Detailed sequences are provided in Table S2.

2.4 | Immunofluorescent study

For CHK1 localisation in the heart, sections were blocked with 5% BSA for 60 min at room temperature. Then, the sections were incubated with primary antibodies against CHK1(1:200) and Actinin (1:100) overnight at 4°C. The next day, the sections were washed and incubated with fluorophore-conjugated secondary antibodies for 1 h. All antibodies were diluted in 1% BSA. Nuclei were stained with DAPI for 5 min, slides were mounted, and images were taken with an epifluorescence microscope (Nikon, Japan).

2.5 | Cell culture and transfection

Neonatal rat cardiomyocytes (NRCMs) were isolated and cultured following the protocol described in our previous study (Wang et al., 2017). Briefly, NRCMs were cultured in Dulbecco's Modified Eagle Medium (DMEM) supplemented with 10% foetal bovine serum (FBS). H9c2 cells (National Collection of Authenticated Cell Cultures, Cat# GNR 5, RRID: CVCL_0286) were used for constructing the H9c2-CHK1 stable knockdown cell line. Briefly, lentiviral transduction (Xu et al., 2022) was used to introduce shRNA targeting CHK1 (sequence: 5′-ccggGAATAACTCACAGGGATATTActcgagTAATATCCC TGTGAGTTATTCttttttg-3′). The cells were cultured with puromycin (2 μg ml^{-1}) for selection. For RNAi, the CHK1 siRNA was obtained from KeyGEN BioTECH (Nanjing, China). For plasmid transfection,

CHK1 S280, S280A and S280E plasmids were obtained from Genechem (Shanghai, China). All transfections were performed using lipofectamine 3000, following the reagent manual.

2.6 | Liquid chromatography with tandem mass spectrometry (LC–MS/MS) proteomics analysis

The potential CHK1-interacting proteins in cells were identified by Co-IP, followed by LC–MS/MS assays. In brief, NRCMs were stimulated with Ang II for 1 h, with saline-treated cells serving as controls. Cell lysates were prepared, and CHK1 protein was immunoprecipitated using an anti-CHK1 antibody and subjected to LC–MS/MS analysis by Applied Protein Technology (Shanghai, China).

2.7 | Echocardiography

Echocardiography was performed using the VINNO 6 Ultrasound System (Suzhou, China) following the manufacturer's instructions. Briefly, mice were anaesthetised with 1.5–2% isoflurane in oxygen, and their chest hair was removed using depilatory cream. Ultrasound gel was applied to the chest of the anaesthetised mice, and parasternal long-axis B-mode images were acquired. M-mode recordings were used to measure left ventricular (LV) wall thickness and dimensions during end-diastole and systole. Throughout the procedure, body temperature was maintained at 37°C, and heart rate was constantly monitored and kept at 450 ± 30 bpm.

2.8 | Measurement of Ang II level

Ang II concentrations in mouse heart tissues were determined using a commercial enzyme-linked immunosorbent assay (ELISA) kit (details in Table S1). Heart tissues were homogenised before measurement. Blood samples were collected, and serum was separated via centrifugation. The serum Ang II levels were measured using the same ELISA kit following the manufacturer's protocol.

2.9 | Histological analysis

Heart tissue pathology was evaluated by dissecting and fixing the hearts in 4% paraformaldehyde. Fixed hearts were sectioned into 5 μm slices and stained with various techniques, including haematoxylin–eosin (H&E), wheat germ agglutinin (WGA), Sirius red and Masson staining. These procedures were performed according to established protocols (Wang et al., 2017).

2.10 | Data and statistical analysis

The data and statistical analysis in this study comply with the recommendations of the British Journal of Pharmacology on experimental design and analysis in pharmacology (Curtis et al., 2025). The group size selection for each protocol is verifiable, and the group size is the number of independent values. All experiments were conducted in a randomised and blinded manner. All the results are presented as mean ± SD from at least five individual values, except for LC–MS/MS proteomics data, which were not subjected to statistical analysis because of small sample sizes (<5), and these results represent our exploratory findings. The exact sample size (*n*) for each experimental group/condition is specified, where '*n*' refers to independent values rather than technical replicates. No exclusion criteria were applied during data collection or analysis. Statistical tests used for each dataset are indicated in the figure legends. All statistical analyses were performed using Prism 10 (GraphPad Software, Boston, USA). Differences between the two groups were assessed using Student's *t*-test. For comparisons involving more than two groups, one-way ANOVA, followed by Dunnett's test was applied. Two-way ANOVA followed by multiple comparisons test was used for experiments with multiple factors. A P value of <0.05 was considered statistically significant. Post hoc tests were run only if F achieved $P < 0.05$, and there was no significant variance inhomogeneity. Specific details are also provided in figure legends.

2.11 | Materials

Ang II (#HY13948A) was supplied by MedChem Express (Shanghai, China), and CCT (# T7080) and UPA (# T7503) were supplied by TargetMol (Shanghai, China). Further details of all reagents, instruments, software, and antibodies used in this study are also provided in Table S1.

2.12 | Nomenclature of targets and ligands

Key protein targets and ligands in this article are hyperlinked to corresponding entries in http://www.guidetopharmacology.org, and are permanently archived in the Concise Guide to PHARMACOLOGY 2023/2024 (Alexander, Christopoulos, et al., 2023; Alexander, Fabbro, et al., 2023).

3 | RESULTS

3.1 | Ang II induces CHK1 S280 phosphorylation in cardiomyocytes

To investigate the role of CHK1 in the progression of cardiac remodelling, we examined the activity of CHK1 in the heart tissues from Ang II-infused mice. Phosphorylation of CHK1 at S345 and S280 have been reported to be responsible for the kinase activation (Capasso et al., 2002; Ma et al., 2019; Morgan et al., 2010). As shown in Figure 1a, neither the total protein level of cardiac CHK1 nor the S345 phosphorylation showed significant changes throughout this experimental period, while CHK1 S280 phosphorylation was time-

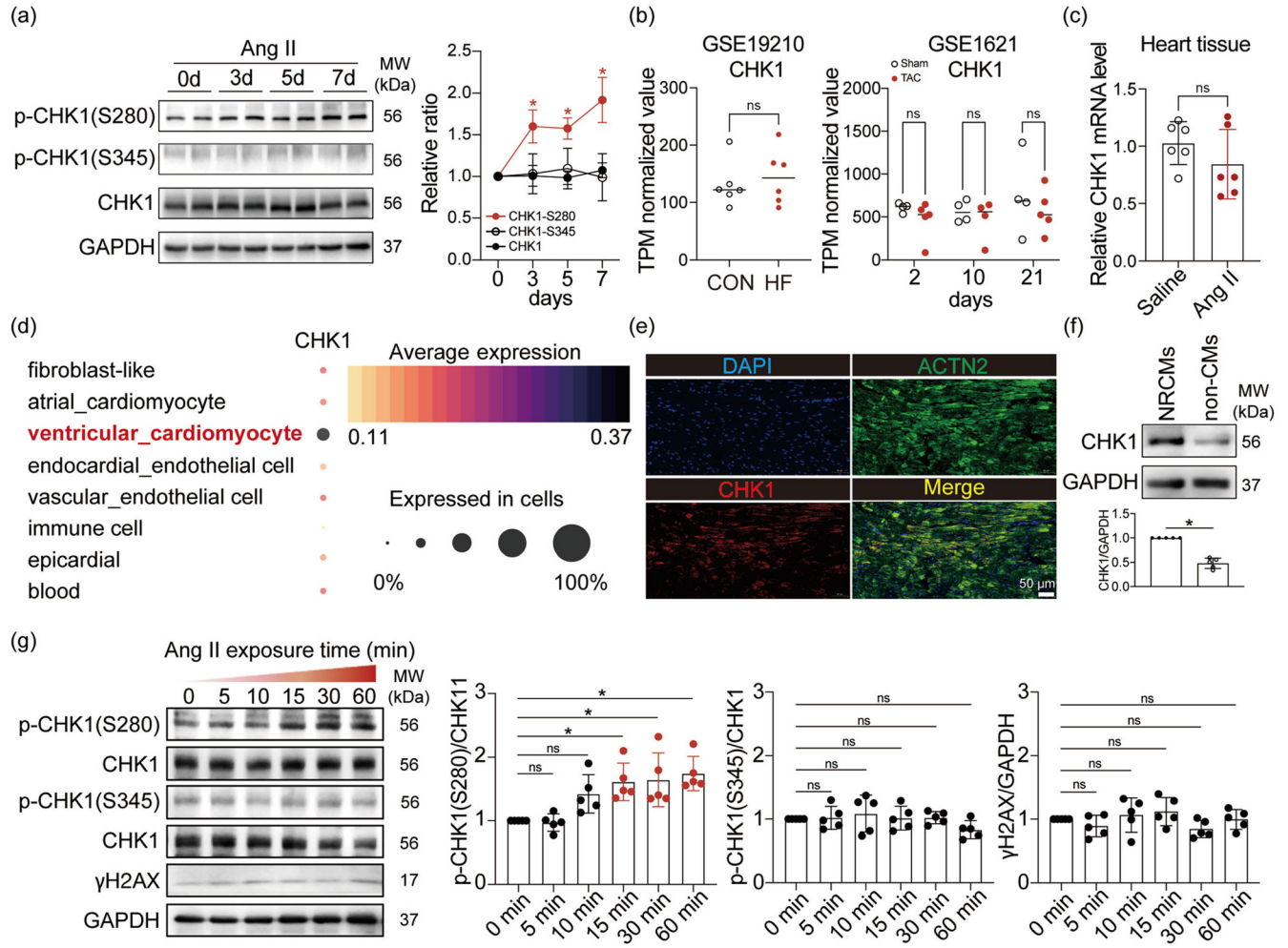

FIGURE 1 **In cardiomyocytes, Ang II induces activation of CHK1 via phosphorylation of S280.** (a) CHK1 phosphorylation levels were evaluated by Western blot in heart tissues from mice infused with Ang II (1000 ng kg^{-1} min^{-1}) for different durations (0, 3, 5 and 7 days). Each group contains three mice. Quantification is shown in the right panel. Data presented are means ± SD, $n = 5$ independent experiments. *P< 0.05, significantly different as indicated; ns, not significant; one-way ANOVA with Dunnett's test. (b) Transcriptional levels of CHK1 in heart tissues were analysed from the GEO database. (c) Relative CHK1 expression in Ang II-infused mouse hearts was measured by quantitative PCR (qPCR). Data presented are means ± SD, $n = 6$. ns, not significantly different as indicated; two-tailed unpaired t-test. (d) CHK1 expression distribution was analysed using single-cell RNA-seq data from mouse hearts (GSE193346). (e) Representative immunostaining of mouse heart samples for CHK1 (red) and cardiomyocyte marker ACTN2 (green), with DAPI (blue) for nuclear staining. Colocalisation of CHK1 and ACTN2 is shown in yellow. Scale bar = 50 μm. (f) Representative Western blot of CHK1 levels in NRCMs and non-CMs. Quantification is shown in the bottom panel. Data presented are means ± SD; $n = 5$ independent experiments. *P< 0.05, significantly different as indicated; two-tailed unpaired t-test. (g) Western blot analysis of p-CHK1 and γH2AX levels in NRCMs treated with Ang II (100 nM) at various time points. The quantification is shown in the right panel. Data presented are means ± SD; $n = 5$ independent experiments. *P< 0.05, significantly different as indicated; ns, not significant; one-way ANOVA with Dunnett's test.

dependently increased in hearts from Ang II-infused mice. Analysis of the GEO database from previous studies (Brooks et al., 2010; Zhao et al., 2004) also showed no significant change in CHK1 transcription levels in the hearts of spontaneous hypertensive rats or mice with transverse aortic coarctation (Figure 1b). Our study also found that Ang II infusion did not affect CHK1 mRNA levels in mouse hearts (Figure 1c). These data indicate that CHK1 S280 phosphorylation, rather than CHK1 expression level, may be associated with Ang II-induced cardiac remodelling. The heart comprises various cell types, including cardiomyocytes, cardiac fibroblasts, endothelial cells and immune cells. To identify the cell types expressing CHK1, a scRNA-seq dataset analysis of mouse heart was used (Feng et al., 2022), which is also available on the UCSC cell browser. The dataset reveals that CHK1 is most abundantly expressed in cardiomyocytes (Figure 1d). Multiple immunofluorescence staining of paraffin-embedded mouse heart tissue further showed the colocalisation of CHK1 with the cardiomyocyte marker, actinin (Figure 1e). Further analysis of primary cardiac cells from the neonatal rats confirmed higher CHK1 protein levels in NRCMs compared to non-cardiomyocytes (Non-CMs, Figure 1f). Based on these results, we

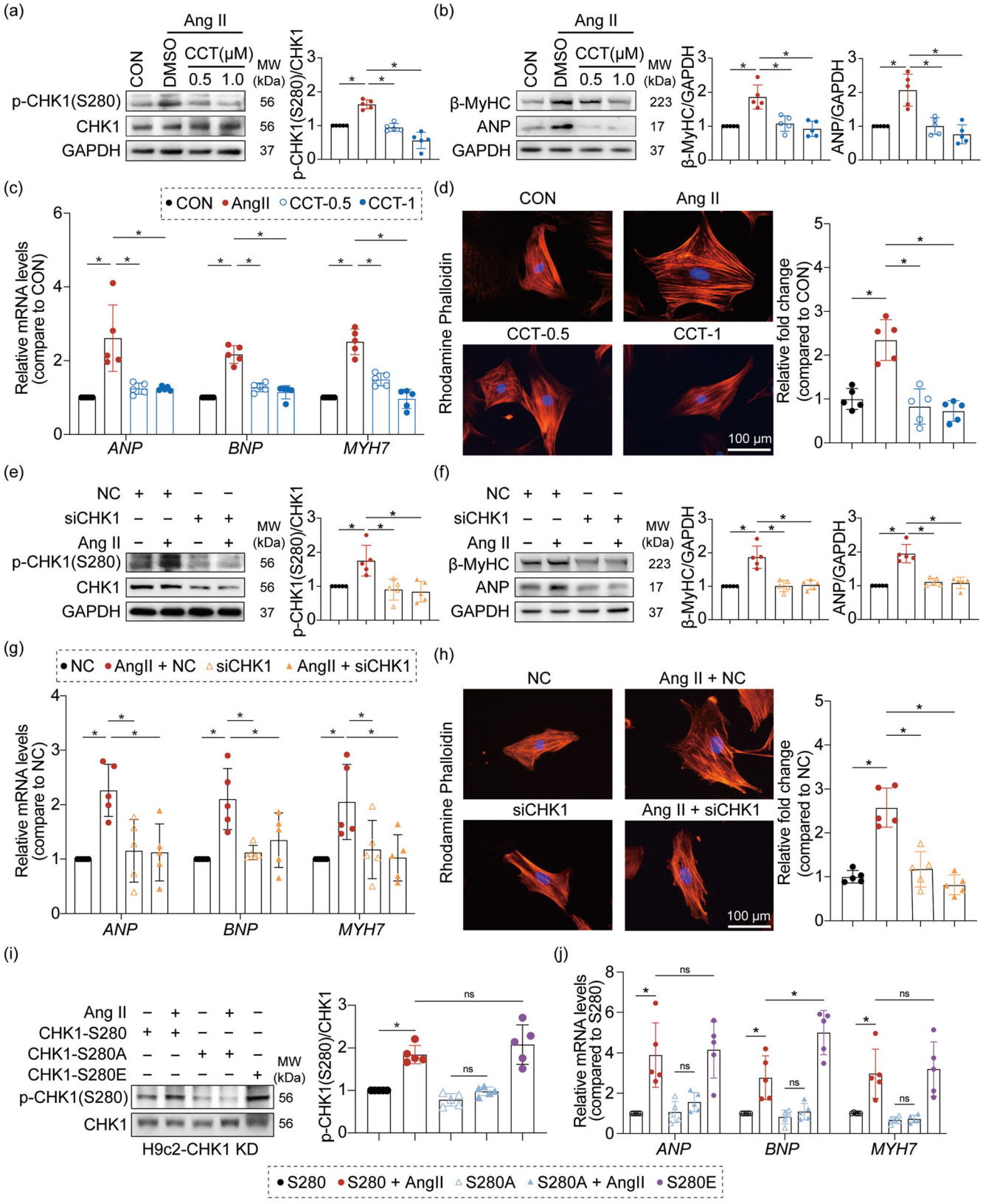

FIGURE 2 Legend on next page.

conclude that CHK1 is predominantly expressed in cardiomyocytes. We then confirmed the selective CHK1 S280 phosphorylation in Ang II-challenged cardiomyocytes. Immunoblotting assay revealed that Ang II challenge failed to induce the phosphorylation of CHK1 S345, as well as the level of γH2AX (Mah et al., 2010), a CHK1-downstream marker of DNA damage, indicating no DNA-level damage in cardiomyocytes (Figure 1g). Similarly, the phosphorylation level of CHK1 S280 was gradually increased by Ang II stimulation in NRCMs (Figure 1g). These findings suggest that Ang II-induced CHK1 S280 phosphorylation may play a role in hypertrophic cardiomyocytes, which may be independent of the better-known DNA damage response.

3.2 | Inhibition of CHK1 S280 alleviates Ang II-induced cardiomyocyte hypertrophy in vitro

The next objective was to determine the functional impact of Ang II-induced CHK1 S280 phosphorylation in cardiomyocytes. To investigate this, we inhibited CHK1 phosphorylation by treating NRCMs with the CHK1 inhibitor **CCT** (Osborne et al., 2016). Based on the cell viability assay conducted at the 24-h time point, we selected concentrations of 0.5 and 1 μmol l^{-1} of CCT for in vitro experiments (Figure S1a). Our findings demonstrate that pretreatment with CCT effectively inhibited Ang II-induced CHK1 S280 phosphorylation in a dose-dependent manner, without affecting the CHK1 protein levels (Figure 2a). CCT pretreatment mitigated the Ang II-induced up-regulation of β-myosin heavy chain (β-MyHC, encoded by MYH7) and **atrial natriuretic peptide (ANP)** protein levels (Horio et al., 2000; Schiaffino et al., 1989) (Figure 2b). Similarly, significant up-regulation of ANP, **brain natriuretic peptide (BNP)** and MYH7 mRNA levels was evident in Ang II-treated NRCMs, which were suppressed by CCT pretreatment (Figure 2c). Cell morphological assessment using rhodamine-phalloidin staining confirmed the attenuation of hypertrophy in CCT-pretreated cells exposed to Ang II (Figure 2d). These data indicate that CHK1 inhibition reduces the hypertrophic responses in Ang II-challenged NRCMs. Additionally, siRNA-mediated CHK1 knockdown (Figure S1b), accompanied by decreased S280 phosphorylation in NRCMs (Figure 2e), also alleviated Ang II-induced cardiomyocyte hypertrophy (Figure 2f–h).

We tried to exclude the involvement of other phosphorylation sites on CHK1. We constructed a phospho-mimetic mutant CHK1 plasmid by substituting serine at position 280 with **glutamic acid** (S280E) to mimic the phosphorylated state (Pearlman et al., 2011). Meanwhile, we generated a CHK1 plasmid by mutating serine 280 to alanine (S280A) to inactivate CHK1 S280. Because of limitations associated with primary cells and the need for sustained observation of pathological changes in cardiomyocytes, we utilised the H9c2 cell line. We established the H9c2 cells with stable CHK1 knockdown (H9c2-CHK1 KD, Figure S1c) and then transfected H9c2-CHK1 KD cells with the mutant plasmids, respectively. Our results showed that substituting serine with alanine or glutamic acid did not affect the CHK1 protein expression. The inactivating mutant CHK1 S280A showed impaired CHK1 phosphorylation response to Ang II, whereas the phospho-mimetic CHK1 S280E mutant exhibited high levels of phosphorylation (Figure 2i). As expected, these alterations influenced the downstream hypertrophic responses. Ang II failed to induce hypertrophy in H9c2 cells with CHK1 S280A, while CHK1 autoactivation by CHK1 S280E transfection alone significantly induced hypertrophy in H9c2 cells (Figures 2j and S1d). These findings confirmed that CHK1 S280 phosphorylation is critical in mediating Ang II-induced cardiomyocyte hypertrophy.

3.3 | Phosphorylation of CHK1 S280 interacts with JAK1 to mediate Ang II-induced cardiomyocyte hypertrophy

We tried to identify the cascade or substrate kinase of CHK1 for its signalling transduction in cardiomyocytes. We performed a screening

FIGURE 2 **Inhibition of CHK1 S280 alleviates Ang II-induced cardiomyocyte hypertrophy in vitro.** (a) NRCMs were pretreated with CCT245737 (CCT) at the indicated concentrations for 1 h before Ang II (100 nM) exposure for 1 h. p-CHK1/CHK1 levels were measured by Western blot. Quantification is shown in the right panel. (b) NRCMs were pretreated with CCT for 1 h before Ang II (100 nM) exposure for 24 h, and β-MyHC and ANP levels were analysed. Quantification is shown in the right panel. (c) NRCMs were pretreated with CCT for 1 h before Ang II (100 nM) exposure for 12 h. The mRNA levels of hypertrophic markers ANP, BNP and MYH7 were determined by qPCR. The transcript levels were normalised to Actb. (d) After CCT treatment and 18 h Ang II (100 nM) exposure, NRCMs were stained with Rhodamine–Phalloidin to detect cardiac myocyte hypertrophy. Scale bar = 100 μm. Quantification is shown in the right panel. (e) NRCMs were transfected with CHK1 siRNA for 24 h before Ang II (100 nM) exposure for 1 h, followed by p-CHK1/CHK1 measurement. Quantification is shown in the right panel. (f) NRCMs were transfected with CHK1 siRNA for 24 h before Ang II (100 nM) exposure for 24 h, and β-MyHC and ANP levels were measured. Quantification is shown in the right panel. (g) NRCMs were transfected with CHK1 siRNA for 24 h before Ang II (100 nM) exposure for 12 h. The mRNA levels of ANP, BNP and MYH7 were determined by qPCR. The transcript levels were normalised to Actb. (h) After siCHK1 transfection and 18 h Ang II exposure, NRCMs were stained with Rhodamine–Phalloidin to detect cardiac myocyte hypertrophy. Scale bar = 100 μm. Quantification is shown in the right panel. (i and j) H9c2 stable CHK1 knockdown cells (H9c2-CHK1 KD) transfected with CHK1 S280/S280A/S280E plasmids as indicated. These cells were exposed to 100 nM Ang II for 1 h or 12 h. (i) The levels of p-CHK1/CHK1 were examined. Quantification is shown in the right panel. (j) The mRNA levels of ANP, BNP and MYH7 were assessed. The transcript levels were normalised to Actb. For Figure 2a,b,d,e,f,h,i, data presented are means ± SD; $n = 5$ independent experiments. *$P < 0.05$, significantly different as indicated; ns, not significant; one-way ANOVA with Dunnett's test. For Figure 2c,g,j, data presented are means ± SD, $n = 5$ independent experiments. *$P < 0.05$, significantly different as indicated; ns, not significant;, two-way ANOVA followed by multiple comparisons test.

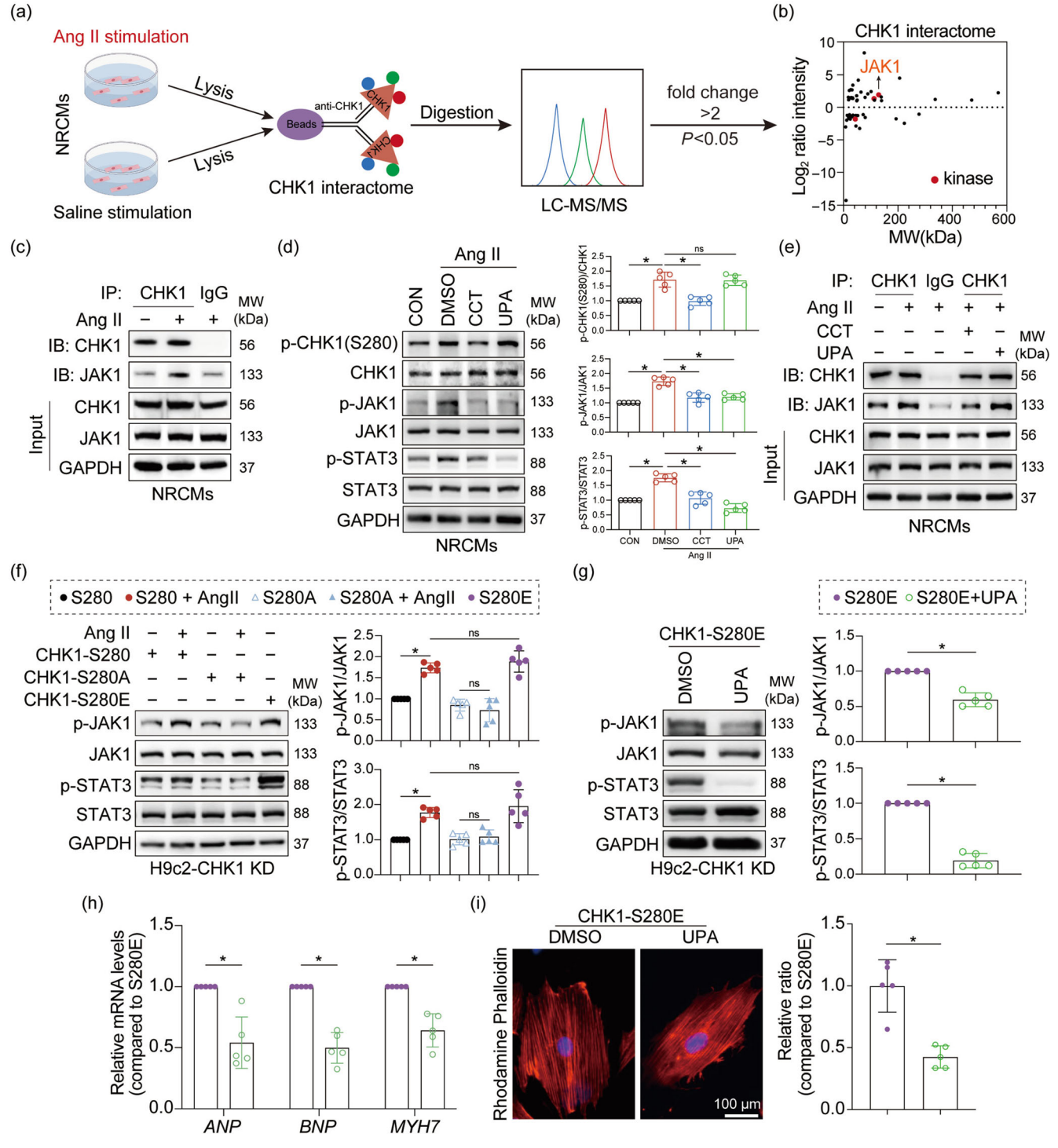

FIGURE 3 Legend on next page.

for potential CHK1 substrate proteins using co-immunoprecipitation (Co-IP) combined with mass spectrometry in NRCMs (Figure 3a). This analysis identified a total of 50 potential CHK1-binding proteins, among which **JAK1**, **Taok1** and Ckm emerged as highly likely kinase candidates (Figures 3b and S2a). Notably, JAK1 (Janus kinase 1) is a key component of the Janus kinase-signal transducer and activator of transcription (JAK–**STAT**) signalling pathway, which is implicated in cardiac remodelling (Barry et al., 2007). Therefore, we hypothesised that JAK1 is the key downstream kinase activated following CHK1 S280 phosphorylation. To validate this hypothesis, we examined the CHK1–JAK1 interaction in Ang II-stimulated NRCMs using Co-IP assay (Figure 3c). We employed the JAK1 inhibitor UPA, and showed that this inhibitor did not affect Ang II-induced CHK1 S280 phosphorylation but significantly inhibited p-JAK1 level, while CCT effectively inhibited the phosphorylation of both CHK1 S280 and JAK1 (Figure 3d). These data suggest that CHK1 functions upstream of JAK1 in this cascade. In addition, the Ang II-induced activation of STAT3, a vital component of the JAK1–STAT3 activation loop (Hu et al., 2021), was inhibited by both CCT and UPA in NRCMs (Figure 3d). Further, Co-IP experiments also confirmed that the CCT significantly suppressed the Ang II-induced complex formation between CHK1 and JAK1, whereas UPA did not influence this interaction (Figure 3e), indicating that CHK1 S280 phosphorylation is necessary for CHK1–JAK1 interaction.

Our next objective was to confirm whether CHK1 S280 phosphorylation mediates the downstream JAK1–STAT3 signalling activation. As shown in Figure 3f, phosphorylation levels of JAK1 and STAT3 were significantly reduced when serine 280 in CHK1 was substituted with alanine. In contrast, the phospho-mimetic CHK1 S280E mutant exhibited elevated levels of p-JAK1 and p-STAT3 (Figure 3f). The defective CHK1 S280A mutant showed decreased CHK1-JAK1 complex formation in response to Ang II, while the autoactivated CHK1 S280E mutant displayed an enhanced binding ability (Figure S2b). Additionally, UPA effectively inhibited both p-JAK1 and p-STAT3 levels (Figure 3g) and suppressed the hypertrophic response induced by the CHK1 S280E mutant (Figure 3h,i). Collectively, these findings suggest that the CHK1 S280–JAK1–STAT3 axis plays a critical role in Ang II-induced cardiomyocyte hypertrophy.

3.4 | Pharmacological inhibition of CHK1 attenuated Ang II-induced cardiac remodelling and dysfunction in mice

Our final objective was to determine whether disrupting CHK1 activity could prevent Ang II-induced cardiac dysfunction. We used a mouse model with continuous Ang II infusion by subcutaneous implant mini-pumps (Xu et al., 2022) and treated these model mice with CCT. In this model, we also used UPA to inhibit JAK1 to confirm the role of the CHK1 S280–JAK1–STAT3 axis in the mouse model. To better evaluate the Ang II-induced cardiac hypertrophy model, we conducted time-course experiments with the Ang II-infused mice (Figure S3). Mice received Ang II infusion for up to 4 weeks, with weekly echocardiographic monitoring. Notably, significant heart enlargement was observed by week 3, with the most pronounced effects evident at week 4, as confirmed by the HW/BW and HW/TL ratios (Figure S3a,b). These data further support the proposal that Ang II infusion induces progressive cardiac dysfunction and remodelling in a time-dependent manner (Figure S3c,d). We also examined the p-CHK1/CHK1 levels in heart tissues of mice with Ang II infusion for 1–4 weeks and found that Ang II infusion also time-dependently induces cardiac CHK1 phosphorylation (Figure S3e). Based on these findings, we selected a 4-week Ang II infusion protocol to establish a robust model of cardiac hypertrophy and remodelling. Both CCT and UPA treatments were administered starting at week 2 to assess their therapeutic efficacy.

During the 4-week Ang II infusion model, we administered CCT and UPA orally to mice starting at week 2. At the end of week 4, we assessed the cardiac function and then killed the mice to collect blood

FIGURE 3 **CHK1 phosphorylated on S280, interacts with JAK1 to mediate Ang II-induced cardiomyocyte hypertrophy.** (a) Schematic representation of the interactome analysis used for screening CHK1 binding proteins. (b) Two-dimensional plot showing $\log_2$ Ang II-CHK1-IP score/saline-CHK1-IP score ratios on the *y*-axis versus protein molecular weight (MW) on the *x*-axis, indicating enrichment of proteins in Ang II-treated NRCMs. (c) Co-immunoprecipitation (Co-IP) of CHK1 and JAK1 in NRCMs treated with or without Ang II. Endogenous CHK1 was immunoprecipitated by anti-CHK1 antibody. IgG served as the control. (d) NRCMs were pretreated with 1 μM CCT or the JAK1 inhibitor upadacitinib (UPA) for 1 h and then exposed to 100 nM Ang II exposure for 1 h. Phosphorylation levels of CHK1, JAK1 and STAT3 were assessed via Western blot, with quantification shown in the right panel. (e) Co-IP of CHK1 and JAK1 in NRCMs treated with either CCT or UPA. (f) H9c2-CHK1 KD cells transfected with CHK1 S280/S280A/S280E plasmids, followed by 100 nM Ang II treatment for 1 h. Phosphorylation levels of JAK1 and STAT3 were examined and quantified in the right panel. (g–i) H9c2-CHK1 KD cells transfected with CHK1 S280E plasmid and treated with UPA. (g) Cells were treated by UPA for 1 h, p-JAK1/JAK1 and p-STAT3/STAT3 were examined, with the quantification in the right panel. (h) After 12 h of UPA treatment, mRNA levels of hypertrophic markers ANP, BNP, and MYH7 were determined by qPCR and normalised to Actb. (i) After 18 h of UPA treatment, NRCMs were stained with Rhodamine–Phalloidin to assess cardiac myocyte hypertrophy. Scale bar = 100 μm, with quantification shown in the right panel. For Figure 3c,e, $n = 5$ independent experiments. For Figure 3d,f, data presented are means ± SD, $n = 5$. independent experiments. *P< 0.05, significantly different as indicated ns, not significant; one-way ANOVA with Dunnett's test. For Figure 3g,i, data presented are means ± SD, $n = 5$ independent experiments. *P< 0.05, significantly different as indicated; Students' *t*-test. For Figure 3h, data presented are means ± SD, $n = 5$ independent experiments. *P< 0.05, significantly different as indicated; two-way ANOVA followed by multiple comparisons test.

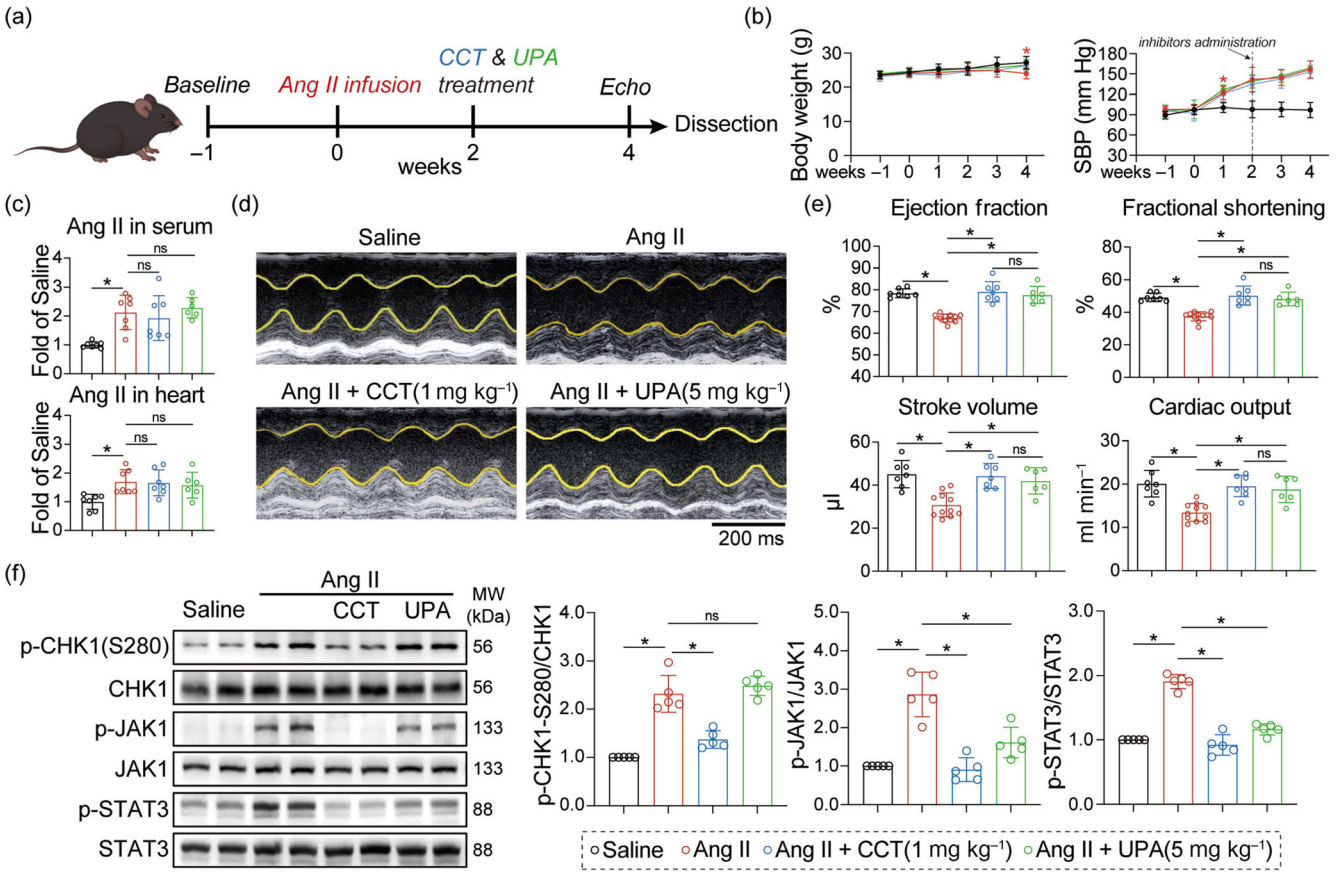

FIGURE 4 **Pharmacological inhibition of CHK1 attenuated Ang II-induced cardiac dysfunction.** (a) Workflow of animal experiment. Ten-week-old male C57bl/6 mice were implanted with subcutaneous minipumps to deliver saline or Ang II and were divided into saline and Ang II groups. CHK1 or JAK1 was inhibited in mice by administering CCT at 1 mg kg^{-1} or UPA at 5 mg kg^{-1} every other day from weeks 2 to 4. Non-invasive echocardiographic assessments were performed to monitor cardiac function after 4 weeks of infusion. (b) Body weight and average systolic blood pressure were measured over the period. Data presented are means ± SD; $n = 6$ to 11. *P< 0.05, significant difference between the WT + Saline group and the WT + Ang II group; two-way ANOVA with multiple comparisons test. (c) Ang II levels in serum and cardiac tissue were assessed using ELISA. (d) Representative M-mode echocardiographic images of the left ventricle. (e) Quantitative analysis of the ejection fraction, fractional shortening, stroke volume and cardiac output. (f) Representative Western blots of p-CHK1, p-JAK1 and p-STAT3 levels in heart tissues. Densitometric quantification is shown in the right panel. Data presented are means ± SD, $n = 5$ independent experiments. *P< 0.05, significantly different as indicated; ns, not significant; one-way ANOVA with Dunnett's test. For Figure 4c,e, data presented are means ± SD, $n = 6$ to 11. *P< 0.05, significantly different as indicated; ns, not significant; one-way ANOVA with Tukey's test.

samples and heart tissue (Figure 4a). As shown in Figure 4b, Ang II infusion resulted in a decrease in body weight at week 4 and a significant increase in systolic blood pressure starting at week 2. Treatment with CCT or UPA reversed the weight loss but did not alter the increase in blood pressure (Figure 4b). Additionally, the administration of CCT or UPA did not affect the Ang II-induced elevation of Ang II levels in serum and heart tissues (Figure 4c). Non-invasive echocardiography revealed significant cardiac function impairment in the Ang II group compared to the saline group, as shown by reduced ejection fraction, fractional shortening, stroke volume and cardiac output (Figure 4d,e and Table S3). Notably, CCT or UPA administration largely reversed the Ang II-induced cardiac dysfunction (Figure 4d,e). However, because of the ageing echocardiography system, image resolution was suboptimal, which may affect the visual representation of group differences. Consistent with the cellular result, pharmacological inhibition of p-CHK1 S280 by CCT successfully decreased JAK1/STAT3 phosphorylation in Ang II-challenged mouse hearts, while UPA failed to decrease CHK1 S280 phosphorylation but still inhibited JAK1 and STAT3 (Figure 4f). Furthermore, the Co-IP results of heart tissues followed a similar trend in CHK1–JAK1 interaction (Figure S4a).

The gross morphology of the hearts and H&E staining of cardiac tissue sections showed that Ang II-induced cardiac hypertrophy was significantly reversed by CCT or UPA treatment (Figure 5a,b). Analysis of the heart weight-to-body weight ratio and the heart weight-to-tibia length ratio further supported this conclusion (Figure 5c). Similar changes were observed in wheat germ agglutinin (WGA) staining of heart sections (Figure 5d,e). Furthermore, compared to the Ang II group, the CCT- and UPA-treated groups exhibited markedly less interstitial fibrosis and collagen accumulation in heart tissues,

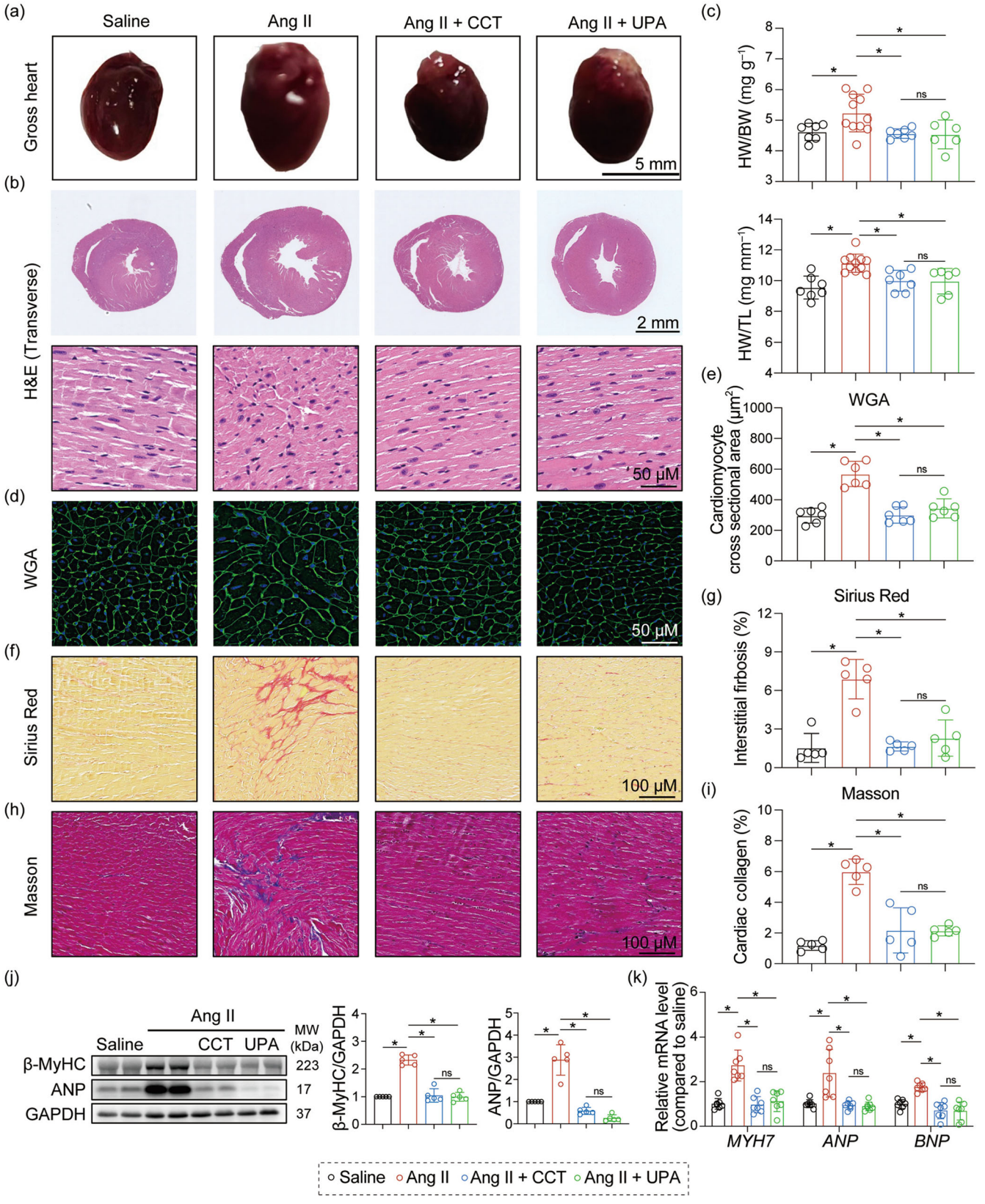

FIGURE 5 Legend on next page.

an outcome of pathological cardiac hypertrophy (Figure 5f–i). Examination of hypertrophic markers, at both protein and mRNA levels, also showed that either CCT or UPA reduced Ang II-induced cardiac hypertrophy (Figure 5j,k). Taken together, these data provide evidence that pharmacological inhibition of the CHK1 S280–JAK1 axis attenuated Ang II-induced cardiac remodelling and dysfunction in mice.

4 | DISCUSSION

In this study, we have explored the role of CHK1 S280 phosphorylation in mediating the pathological processes of Ang II-induced cardiac remodelling. We found that CHK1 S280 phosphorylation recruited JAK1 protein, which in turn phosphorylated JAK1 and thereby activated the JAK1/STAT3 pathway to induce hypertrophy in cardiomyocytes. Pharmacological inhibition of CHK1 activity significantly attenuated cardiac dysfunction and remodelling. These findings highlight the importance of CHK1 S280 phosphorylation in Ang II-induced cardiac injury.

Previous studies on CHK1 have primarily focussed on its role in cell proliferation and DDR, where it is activated in response to replication stress (Dai & Grant, 2010; Patil et al., 2013). This activation triggers downstream pathways that contribute to disease development, especially cancers. In cancer, abnormal DNA replication stress leads to CHK1 activation, enabling tumour cells to repair their DNA and to continue proliferating (Dai & Grant, 2010). Similarly, in non-oncological research, ROS-induced DDR in renal ischaemia–reperfusion activated CHK1 (Ajay et al., 2014). In DDR-induced CHK1 activation, the phosphorylation at S345 is canonical and essential (Patil et al., 2013). In addition, Yuan et al. reported selective CHK1 S280 activation without affecting S345 phosphorylation in acute myeloid leukaemia (Yuan et al., 2014), and another study explored the special role of CHK1 S280 phosphorylation during mitosis (Adam et al., 2018). Generally, in the proliferative or DNA-repair functions, S345 phosphorylation regulates substrates such as CDC 25 and **WEE1** to induce cell cycle arrest (Tapia-Alveal et al., 2009), S280 phosphorylation promotes CHK1 nuclear translocation and then contributes to genome stability (Nguyen et al., 2023; Puc et al., 2005).

However, the specific pathways mediated by different serine sites in CHK1, especially in non-canonical roles, such as cardiac remodelling, remain an area requiring further investigation. Interestingly, in our study, we found that the phosphorylation of CHK1 S280, but not CHK1 S345, was significantly responsive to Ang II stimulation without any change in the level of γH2AX (an early marker of DNA double-strand breaks). An interesting concern is that a majority of cardiomyocytes are terminally differentiated. Adult cardiomyocytes show very limited proliferative capacity and cell cycle activity (Zhu et al., 2024). Based on our findings, CHK1 plays a unique role beyond the conventional proliferation and DDR, with S280 phosphorylation and subsequent regulation of JAK1-STAT3 signalling in regulating cardiac remodelling. This study showed that S280 phosphorylation of CHK1 in terminally differentiated cardiomyocytes was independent of cell cycle and proliferation regulation. This study also opens a new avenue for understanding the differential activation of CHK1 serine sites and highlights the potential for targeting S280 phosphorylation in heart diseases.

Research on CHK1 in cardiology has been relatively limited. Recently, Wang's team has studied its role in myocardial repair and regeneration (Fan et al., 2020; Wei et al., 2024). They identified CHK1 as a key kinase in myocardial repair through quantitative phosphorylated proteomics of infarcted neonatal mice hearts (Fan et al., 2020). Overexpression of CHK1 promoted cardiomyocyte proliferation and improved heart function after infarction (Fan et al., 2020). Their research extended to porcine models of myocardial ischaemia/reperfusion, where CHK1 hydrogel effectively restored heart function (Wei et al., 2024). In these earlier studies, however, myocardial infarction increased the total CHK1 level, but S345 phosphorylation remained unchanged, with S317 serving as the activation marker (Fan et al., 2020; Wei et al., 2024); however, the S280 phosphorylation was not detected. Collectively, this reinforces our hypothesis that distinct CHK1 phosphorylation sites mediate different signalling pathways.

The JAK1–STAT3 pathway is a well-known signalling cascade involved in the regulation of cardiac remodelling and heart failure (Baldini et al., 2021; Booz et al., 2002; Terrell et al., 2006). Through Co-IP/MS analyses, we identified JAK1 as a direct interacting partner of CHK1 in cardiomyocytes. Further analysis using small-molecule

FIGURE 5 **Pharmacological inhibition of CHK1 attenuated Ang II-induced cardiac hypertrophy and fibrosis.** (a) Representative images of gross heart morphology from each group. Scale bar = 5 mm. (b) Representative H&E-stained cardiac sections showing structural changes. Upper scale bar = 2 mm; lower scale bar = 50 μm. (c) Heart weight to body weight (HW/BW, upper panel) ratio and heart weight to tibia length (HW/TL, lower panel) ratio. Data are presented as mean ± SD, $n = 6$ to 11, and P-values were calculated by one-way ANOVA with Dunnett's test. (d and e) Representative wheat germ agglutinin (WGA) staining for cardiomyocyte cross-sectional area in heart sections. Scale bar = 50 μm. Figure 5e shows the quantification of the cardiomyocyte area in each group. (f and g) Representative images of Sirius red-stained heart sections. Scale bar = 100 μm. Figure 5g shows the quantification of the interstitial fibrosis. (h and i) Representative images of Masson-stained heart sections. Scale bar = 100 μm. Figure 5i shows the quantification of the cardiac collagen deposit. (j) The protein levels of hypertrophic markers β-MyHC and ANP were determined by Western blot. Quantification is shown in the right panel. Data presented are means ± SD, $n = 5$. *P< 0.05, significantly different as indicated; ns, not significant; one-way ANOVA with Dunnett's test. (k) The mRNA levels of ANP, BNP and MYH7 were determined by qPCR. Data are presented are means ± SD, $n = 7$. *P< 0.05, significantly different as indicated; ns, not significant; two-way ANOVA followed by multiple comparisons test. For Figure 5e,g,i data presented are means ± SD, $n = 5$. *P< 0.05, significantly different as indicated, ns, not significant; one-way ANOVA with Dunnett's test.

inhibitors and mutant plasmids confirmed that CHK1 acts as an upstream kinase in the CHK1–JAK1 signalling axis. Typically, ligand-activated cytokine receptors or G-protein coupled receptors (GPCRs) can recruit JAK1, which phosphorylates and activates STAT3, driving downstream signalling and pro-hypertrophic gene transcription (Bousoik & Montazeri Aliabadi, 2018; Chang et al., 2002; Hu et al., 2021). Numerous studies have confirmed the crucial role of STAT3 in pathological cardiac hypertrophy (Fischer & Hilfiker-Kleiner, 2007). As a DNA-binding transcriptional activator, STAT3 directly binds to hypertrophic and pro-fibrotic gene promoters to up-regulate the transcription and expression of proteins related to cardiac remodelling, such as MyHC, ANP, **Collagen-1** and **TGF-β** in cardiomyocytes (Han et al., 2018; Ye et al., 2020). Therapeutic strategies targeting STAT3 to treat cardiac hypertrophy have recently emerged (Ye et al., 2020). Our results suggest that CHK1–JAK1 interaction directly activates JAK1, leading to STAT3 activation and hypertrophic phenotypes in cardiomyocytes. To our knowledge, we present the first demonstration that CHK1 S280 phosphorylation directly regulates JAK1, suggesting a novel CHK1–JAK1–STAT3 pathway in cardiac hypertrophy.

One limitation of this study should be acknowledged; although we identified JAK1 as a downstream kinase of CHK1, other kinases, such as Taok1 and Ckm, found in our Co-IP/MS experiments, were not explored in depth. Taok1 is a serine/threonine kinase involved in MAPK signalling (Li et al., 2024). Recent studies suggest that Taok1 participates in LPS-induced inflammatory (Zhu et al., 2020) and **doxorubicin**-induced cardiac injury (Suga et al., 2025; Zhou et al., 2024), which may affect the myocardium under pathological stress. Additionally, Ckm, traditionally known for its role in maintaining ATP homeostasis in muscle tissue (Veksler et al., 1995), has also been implicated in cardiac energy metabolism and contractile function (Keceli et al., 2022). The Co-IP/MS data including Taok1 and Ckm raises the possibility that cardiomyocyte CHK1 may also regulate other kinase pathways in addition to the JAK1–STAT3 axis, potentially contributing to cardiac remodelling. Besides, CHK1–Ckm interaction might reflect a potential role in myocardial energy regulation, particularly under Ang II stimulation. These associations suggest a broader regulatory network downstream of CHK1 in cardiomyocytes, which deserves further investigation. Another unresolved question in this study is how Ang II induces CHK1 activation at S280. Because CHK1 is predominantly localised in the cytosol and nucleus (Wang et al., 2012), the involvement of a membrane receptor of Ang II, for example, **AT_1 receptors**, in its activation is plausible. Although Pim1/2 (Yuan et al., 2014), **Akt** (Adam et al., 2018) and p90 ribosomal S6 kinase (Li et al., 2012) have been reported to regulate CHK1 S280 phosphorylation, it is unclear whether Ang II activates CHK1 at S280 through its classical AT_1 receptors and these previously reported upstream kinases. Further investigation of this mechanism is essential for understanding the specific role of CHK1 S280 activation in cardiomyocytes.

In conclusion, our study has identified CHK1 S280 phosphorylation as a novel mediator of Ang II-induced cardiomyocyte hypertrophy and cardiac dysfunction. The CHK1 S280–JAK1–STAT3 axis plays a critical role in driving these pathological processes, and pharmacological inhibition of this pathway represents a promising therapeutic strategy for preventing hypertensive heart failure. These findings contribute to a better understanding of the molecular mechanisms underlying cardiac hypertrophy and open new avenues for the development of targeted therapies.

AUTHOR CONTRIBUTIONS

Z. Xu: Conceptualisation (lead); data curation (supporting); formal analysis (lead); funding acquisition (lead); investigation (equal); methodology (supporting); project administration (lead); visualisation (lead); writing—original draft (lead); writing—review and editing (equal). **Y. Shen**: Data curation (lead); investigation (equal); methodology (equal); validation (lead); visualisation (supporting). **X. Luo**: Funding acquisition (supporting); investigation (equal); resources (equal); validation (equal). **J. Wang**: Data curation (equal); investigation (equal); methodology (equal). **Q. Zhou**: Data curation (equal); methodology (equal); validation (equal). **X. Han**: Resources (equal); software (equal). **J. Ren**: Project administration (supporting); resources (supporting). **L. Wang**: Resources (supporting); supervision (supporting). **G. Liang**: Conceptualisation (supporting); resources (lead); software (lead); supervision (lead); writing—review and editing (equal).

ACKNOWLEDGEMENTS

This work was supported by the National Natural Science Foundation of China (82300532 to Z.X.), the Natural Science Foundation of Zhejiang Province (LQ22H020002 to Z.X.), the Medical and Health Research Project of Zhejiang Province (2025KY023 to X.L.) and the Fundamental Research Funds for the Hangzhou Medical College (KYZD2023004 to Z.X.).

CONFLICT OF INTERESTS STATEMENT

The authors declare no conflicts of interest.

DATA AVAILABILITY STATEMENT

The data that support the findings of this study are available from the corresponding author.

DECLARATION OF TRANSPARENCY AND SCIENTIFIC RIGOUR

This Declaration acknowledges that this paper adheres to the principles for transparent reporting and scientific rigour of preclinical research as stated in the *BJP* guidelines for Design and Analysis, Immunoblotting and Immunochemistry, and Animal Experimentation, and as recommended by funding agencies, publishers and other organisations engaged with supporting research.

ORCID

Zheng Xu https://orcid.org/0000-0002-8945-3107
Guang Liang https://orcid.org/0009-0005-1603-3223

REFERENCES

Adam, K., Cartel, M., Lambert, M., David, L., Yuan, L., Besson, A., Mayeux, P., Manenti, S., & Didier, C. (2018). A PIM-CHK1 signaling

pathway regulates PLK1 phosphorylation and function during mitosis. *Journal of Cell Science*, *131*, jcs213116. https://doi.org/10.1242/jcs.213116

Ajay, A. K., Kim, T. M., Ramirez-Gonzalez, V., Park, P. J., Frank, D. A., & Vaidya, V. S. (2014). A bioinformatics approach identifies signal transducer and activator of transcription-3 and checkpoint kinase 1 as upstream regulators of kidney injury molecule-1 after kidney injury. *Journal of the American Society of Nephrology: JASN*, *25*, 105–118. https://doi.org/10.1681/ASN.2013020161

Alexander, S. P. H., Christopoulos, A., Davenport, A. P., Kelly, E., Mathie, A. A., Peters, J. A., Veale, E. L., Armstrong, J. F., Faccenda, E., Harding, S. D., Davies, J. A., Abbracchio, M. P., Abraham, G., Agoulnik, A., Alexander, W., Al-hosaini, K., Bäck, M., Baker, J. G., Barnes, N. M., … Ye, R. D. (2023). The Concise Guide to PHARMACOLOGY 2023/24: G protein-coupled receptors. *British Journal of Pharmacology*, *180*(Suppl 2), S23–S144. https://doi.org/10.1111/bph.16177

Alexander, S. P. H., Fabbro, D., Kelly, E., Mathie, A. A., Peters, J. A., Veale, E. L., Armstrong, J. F., Faccenda, E., Harding, S. D., Davies, J. A., Annett, S., Boison, D., Burns, K. E., Dessauer, C., Gertsch, J., Helsby, N. A., Izzo, A. A., Ostrom, R., Papapetropoulos, A., … Wong, S. S. (2023). The Concise Guide to PHARMACOLOGY 2023/24: Enzymes. *British Journal of Pharmacology*, *180*(Suppl 2), S289–S373. https://doi.org/10.1111/bph.16181

Alexander, S. P. H., Roberts, R. E., Broughton, B. R. S., Sobey, C. G., George, C. H., Stanford, S. C., Cirino, G., Docherty, J. R., Giembycz, M. A., Hoyer, D., Insel, P. A., Izzo, A. A., Ji, Y., MacEwan, D., Mangum, J., Wonnacott, S., & Ahluwalia, A. (2018). Goals and practicalities of immunoblotting and immunohistochemistry: A guide for submission to the British Journal of Pharmacology. *British Journal of Pharmacology*, *175*, 407–411. https://doi.org/10.1111/bph.14112

Baldini, C., Moriconi, F. R., Galimberti, S., Libby, P., & De Caterina, R. (2021). The JAK-STAT pathway: an emerging target for cardiovascular disease in rheumatoid arthritis and myeloproliferative neoplasms. *European Heart Journal*, *42*, 4389–4400. https://doi.org/10.1093/eurheartj/ehab447

Barry, S. P., Townsend, P. A., Latchman, D. S., & Stephanou, A. (2007). Role of the JAK-STAT pathway in myocardial injury. *Trends in Molecular Medicine*, *13*, 82–89.

Booz, G. W., Day, J. N., & Baker, K. M. (2002). Interplay between the cardiac renin angiotensin system and JAK-STAT signaling: role in cardiac hypertrophy, ischemia/reperfusion dysfunction, and heart failure. *Journal of Molecular and Cellular Cardiology*, *34*, 1443–1453.

Borenas, M., Umapathy, G., Lind, D. E., Lai, W. Y., Guan, J., Johansson, J., Jennische, E., Schmidt, A., Kurhe, Y., Gabre, J. L., & Aniszewska, A. (2024). ALK signaling primes the DNA damage response sensitizing ALK-driven neuroblastoma to therapeutic ATR inhibition. *Proceedings of the National Academy of Sciences of the United States of America*, *121*, e2315242121.

Bousoik, E., & Montazeri Aliabadi, H. (2018). "Do we know Jack" about JAK? A closer look at JAK/STAT signaling pathway. *Frontiers in Oncology*, *8*, 287.

Brooks, W. W., Shen, S. S., Conrad, C. H., Goldstein, R. H., & Bing, O. H. (2010). Transition from compensated hypertrophy to systolic heart failure in the spontaneously hypertensive rat: Structure, function, and transcript analysis. *Genomics*, *95*, 84–92. https://doi.org/10.1016/j.ygeno.2009.12.002

Capasso, H., Palermo, C., Wan, S., Rao, H., John, U. P., O'Connell, M. J., & Walworth, N. C. (2002). Phosphorylation activates Chk1 and is required for checkpoint-mediated cell cycle arrest. *Journal of Cell Science*, *115*, 4555–4564.

Chang, Y. J., Holtzman, M. J., & Chen, C. C. (2002). Interferon-gamma-induced epithelial ICAM-1 expression and monocyte adhesion. Involvement of protein kinase C-dependent c-Src tyrosine kinase activation pathway. *Journal of Biological Chemistry*, *277*, 7118–7126.

Curtis, M. J., Alexander, S. P. H., Cortese-Krott, M., Kendall, D. A., Martemyanov, K. A., Mauro, C., Panettieri, R. A. Jr., Papapetropoulos, A., Patel, H. H., Santo, E. E., Schulz, R., Stefanska, B., Stephens, G. J., Teixeira, M. M., Vergnolle, N., Wang, X., & Ferdinandy, P. (2025). Guidance on the planning and reporting of experimental design and analysis. *British Journal of Pharmacology*, *182*, 1413–1415. https://doi.org/10.1111/bph.17441

Dai, Y., & Grant, S. (2010). New insights into checkpoint kinase 1 in the DNA damage response signaling network. *Clinical Cancer Research*, *16*, 376–383. https://doi.org/10.1158/1078-0432.CCR-09-1029

Fan, Y., Cheng, Y., Li, Y., Chen, B., Wang, Z., Wei, T., Zhang, H., Guo, Y., Wang, Q., Wei, Y., Chen, F., Sha, J., Guo, X., & Wang, L. (2020). Phosphoproteomic analysis of neonatal regenerative myocardium revealed important roles of checkpoint kinase 1 via activating mammalian target of rapamycin C1/ribosomal protein S6 kinase b-1 pathway. *Circulation*, *141*, 1554–1569. https://doi.org/10.1161/CIRCULATIONAHA.119.040747

Feng, W., Bais, A., He, H., Rios, C., Jiang, S., Xu, J., Chang, C., Kostka, D., & Li, G. (2022). Single-cell transcriptomic analysis identifies murine heart molecular features at embryonic and neonatal stages. *Nature Communications*, *13*, 7960.

Fischer, P., & Hilfiker-Kleiner, D. (2007). Survival pathways in hypertrophy and heart failure: the gp130-STAT3 axis. *Basic Research in Cardiology*, *102*, 279–297.

Forrester, S. J., Booz, G. W., Sigmund, C. D., Coffman, T. M., Kawai, T., Rizzo, V., Scalia, R., & Eguchi, S. (2018). Angiotensin II signal transduction: An update on mechanisms of physiology and pathophysiology. *Physiological Reviews*, *98*, 1627–1738. https://doi.org/10.1152/physrev.00038.2017

Frangogiannis, N. G. (2021). Cardiac fibrosis. *Cardiovascular Research*, *117*, 1450–1488. https://doi.org/10.1093/cvr/cvaa324

Frantz, S., Hundertmark, M. J., Schulz-Menger, J., Bengel, F. M., & Bauersachs, J. (2022). Left ventricular remodelling post-myocardial infarction: pathophysiology, imaging, and novel therapies. *European Heart Journal*, *43*, 2549–2561. https://doi.org/10.1093/eurheartj/ehac223

Gioia, U., Tavella, S., Martinez-Orellana, P., Cicio, G., Colliva, A., Ceccon, M., Cabrini, M., Henriques, A. C., Fumagalli, V., Paldino, A., & Presot, E. (2023). SARS-CoV-2 infection induces DNA damage, through CHK1 degradation and impaired 53BP1 recruitment, and cellular senescence. *Nature Cell Biology*, *25*, 550–564.

Han, J., Ye, S., Zou, C., Chen, T., Wang, J., Li, J., Jiang, L., Xu, J., Huang, W., Wang, Y., & Liang, G. (2018). Angiotensin II causes biphasic STAT3 activation through TLR4 to initiate cardiac remodeling. *Hypertension (Dallas, Tex: 1979)*, *72*, 1301–1311.

Horio, T., Nishikimi, T., Yoshihara, F., Matsuo, H., Takishita, S., & Kangawa, K. (2000). Inhibitory regulation of hypertrophy by endogenous atrial natriuretic peptide in cultured cardiac myocytes. *Hypertension (Dallas, Tex: 1979)*, *35*, 19–24.

Hu, X., Li, J., Fu, M., Zhao, X., & Wang, W. (2021). The JAK/STAT signaling pathway: From bench to clinic. *Signal Transduction and Targeted Therapy*, *6*, 402.

Jiang, K., Deng, M., Du, W., Liu, T., Li, J., & Zhou, Y. (2024). Functions and inhibitors of CHK1 in cancer therapy. *Medicine in Drug Discovery*, *22*, 100185.

Keceli, G., Gupta, A., Sourdon, J., Gabr, R., Schar, M., Dey, S., Tocchetti, C. G., Stuber, A., Agrimi, J., Zhang, Y., & Leppo, M. (2022). Mitochondrial creatine kinase attenuates pathologic remodeling in heart failure. *Circulation Research*, *130*, 741–759.

Li, J., Wei, X., Dong, Z., Fu, Y., Ma, Y., & Hailong, W. (2024). Research progress on anti-tumor mechanism of TAOK kinases. *Cellular Signalling*, *124*, 111385.

Li, P., Goto, H., Kasahara, K., Matsuyama, M., Wang, Z., Yatabe, Y., Kiyono, T., & Inagaki, M. (2012). P90 RSK arranges Chk1 in the nucleus for monitoring of genomic integrity during cell proliferation. *Molecular Biology of the Cell*, *23*, 1582–1592. https://doi.org/10.1091/mbc.E11-10-0883

Lilley, E., Stanford, S. C., Kendall, D. E., Alexander, S. P. H., Cirino, G., Docherty, J. R., George, C. H., Insel, P. A., Izzo, A. A., Ji, Y., Panettieri, R. A., Sobey, C. G., Stefanska, B., Stephens, G., Teixeira, M. M., & Ahluwalia, A. (2020). ARRIVE 2.0 and the British Journal of Pharmacology: Updated guidance for 2020. *British Journal of Pharmacology*, *177*, 3611–3616. https://doi.org/10.1111/bph.15178

Ma, Y., Cui, D., Xiong, X., Inuzuka, H., Wei, W., Sun, Y., North, B. J., & Zhao, Y. (2019). SCFbeta-TrCP ubiquitinates CHK1 in an AMPK-dependent manner in response to glucose deprivation. *Molecular Oncology*, *13*, 307–321.

Mah, L. J., El-Osta, A., & Karagiannis, T. C. (2010). gammaH2AX: A sensitive molecular marker of DNA damage and repair. *Leukemia*, *24*, 679–686. https://doi.org/10.1038/leu.2010.6

Martin, T. G., Juarros, M. A., & Leinwand, L. A. (2023). Regression of cardiac hypertrophy in health and disease: mechanisms and therapeutic potential. *Nature Reviews. Cardiology*, *20*, 347–363. https://doi.org/10.1038/s41569-022-00806-6

Morgan, M. A., Parsels, L. A., Zhao, L., Parsels, J. D., Davis, M. A., Hassan, M. C., Arumugarajah, S., Hylander-Gans, L., Morosini, D., Simeone, D. M., Canman, C. E., Normolle, D. P., Zabludoff, S. D., Maybaum, J., & Lawrence, T. S. (2010). Mechanism of radiosensitization by the Chk1/2 inhibitor AZD7762 involves abrogation of the G2 checkpoint and inhibition of homologous recombinational DNA repair. *Cancer Research*, *70*, 4972–4981. https://doi.org/10.1158/0008-5472.CAN-09-3573

Nguyen, M. T. H., Imanishi, M., Li, S., Chau, K., Banerjee, P., Velatooru, L. R., Ko, K. A., Samanthapudi, V. S. K., Gi, Y. J., Lee, L. L., Abe, R. J., McBeath, E., Deswal, A., Lin, S. H., Palaskas, N. L., Dantzer, R., Fujiwara, K., Borchrdt, M. K., Turcios, E. B., … Le, N. T. (2023). Endothelial activation and fibrotic changes are impeded by laminar flow-induced CHK1-SENP2 activity through mechanisms distinct from endothelial-to-mesenchymal cell transition. *Frontiers in Cardiovascular Medicine*, *10*, 1187490.

Osborne, J. D., Matthews, T. P., McHardy, T., Proisy, N., Cheung, K. M., Lainchbury, M., Brown, N., Walton, M. I., Eve, P. D., Boxall, K. J., & Hayes, A. (2016). Multiparameter lead optimization to give an oral checkpoint kinase 1 (CHK1) inhibitor clinical candidate: (R)-5-((4-([Morpholin-2-ylmethyl]amino)-5-(trifluoromethyl)pyridin-2-yl) amino)pyrazine-2-carbonitrile (CCT245737). *Journal of Medicinal Chemistry*, *59*, 5221–5237.

Patil, M., Pabla, N., & Dong, Z. (2013). Checkpoint kinase 1 in DNA damage response and cell cycle regulation. *Cellular and Molecular Life Sciences*, *70*, 4009–4021. https://doi.org/10.1007/s00018-013-1307-3

Pearlman, S. M., Serber, Z., & Ferrell, J. E. Jr. (2011). A mechanism for the evolution of phosphorylation sites. *Cell*, *147*, 934–946. https://doi.org/10.1016/j.cell.2011.08.052

Percie du Sert, N., Hurst, V., Ahluwalia, A., Alam, S., Avey, M. T., Baker, M., Browne, W. J., Clark, A., Cuthill, I. C., Dirnagl, U., Emerson, M., Garner, P., Holgate, S. T., Howells, D. W., Karp, N. A., Lazic, S. E., Lidster, K., MacCallum, C. J., Macleod, M., … Würbel, H. (2020). The ARRIVE guidelines 2.0: updated guidelines for reporting animal research. *PLoS Biology*, *18*, e3000410. https://doi.org/10.1371/journal.pbio.3000410

Puc, J., Keniry, M., Li, H. S., Pandita, T. K., Choudhury, A. D., Memeo, L., Mansukhani, M., Murty, V. V., Gaciong, Z., Meek, S. E., Piwnica-Worms, H., Hibshoosh, H., & Parsons, R. (2005). Lack of PTEN sequesters CHK1 and initiates genetic instability. *Cancer Cell*, *7*, 193–204.

Schiaffino, S., Samuel, J. L., Sassoon, D., Lompre, A. M., Garner, I., Marotte, F., Buckingham, M., Rappaport, L., & Schwartz, K. (1989). Nonsynchronous accumulation of alpha-skeletal actin and beta-myosin heavy chain mRNAs during early stages of pressure-overload-induced cardiac hypertrophy demonstrated by in situ hybridization. *Circulation Research*, *64*, 937–948.

Suga, T., Kitani, T., Kogure, M., Oishi, M., Ito, F., Hoshino, A., Ogata, T., Ikeda, K., & Matoba, S. (2025). TAOK1 suppression improves doxorubicin-induced cardiomyopathy by preventing cardiomyocyte death and dysfunction. *Cardiovascular Research*, *121*, 601–613.

Tapia-Alveal, C., Calonge, T. M., & O'Connell, M. J. (2009). Regulation of chk1. *Cell Div*, *4*, 8.

Terrell, A. M., Crisostomo, P. R., Wairiuko, G. M., Wang, M., Morrell, E. D., & Meldrum, D. R. (2006). Jak/STAT/SOCS signaling circuits and associated cytokine-mediated inflammation and hypertrophy in the heart. *Shock (Augusta, Ga)*, *26*, 226–234.

Veksler, V. I., Kuznetsov, A. V., Anflous, K., Mateo, P., van Deursen, J., Wieringa, B., & Ventura-Clapier, R. (1995). Muscle creatine kinase-deficient mice. II. Cardiac and skeletal muscles exhibit tissue-specific adaptation of the mitochondrial function. *The Journal of Biological Chemistry*, *270*, 19921–19929.

Wang, J., Han, X., Feng, X., Wang, Z., & Zhang, Y. (2012). Coupling cellular localization and function of checkpoint kinase 1 (Chk1) in checkpoints and cell viability. *The Journal of Biological Chemistry*, *287*, 25501–25509. https://doi.org/10.1074/jbc.M112.350397

Wang, Y., Qian, Y., Fang, Q., Zhong, P., Li, W., Wang, L., Fu, W., Zhang, Y., Xu, Z., Li, X., & Liang, G. (2017). Saturated palmitic acid induces myocardial inflammatory injuries through direct binding to TLR4 accessory protein MD2. *Nature Communications*, *8*, 13997.

Wei, T. W., Shan, T. K., Wang, H., Chen, J. W., Yang, T. T., Zhou, L. H., Zhao, D., Sun, J. T., Wang, S. B., Gu, L. F., & Du, C. (2024). Checkpoint kinase 1 stimulates endogenous cardiomyocyte renewal and cardiac repair by binding to pyruvate kinase isoform M2 C-domain and activating cardiac metabolic reprogramming in a porcine model of myocardial ischemia/reperfusion injury. *Journal of the American Heart Association*, *13*, e034805.

Xu, Z., Luo, W., Chen, L., Zhuang, Z., Yang, D., Qian, J., Khan, Z. A., Guan, X., Wang, Y., Li, X., & Liang, G. (2022). Ang II (angiotensin II)-induced FGFR1 (fibroblast growth factor receptor 1) activation in tubular epithelial cells promotes hypertensive kidney fibrosis and injury. *Hypertension (Dallas, Tex: 1979)*, *79*, 2028–2041.

Yang, T. T., Zhou, L. H., Gu, L. F., Qian, L. L., Bao, Y. L., Jing, P., Sun, J. T., Du, C., Shan, T. K., Wang, S. B., & Wang, W. J. (2025). CHK1 attenuates cardiac dysfunction via suppressing SIRT1-ubiquitination. *Metabolism*, *162*, 156048.

Ye, S., Luo, W., Khan, Z. A., Wu, G., Xuan, L., Shan, P., Lin, K., Chen, T., Wang, J., Hu, X., Wang, S., Huang, W., & Liang, G. (2020). Celastrol attenuates angiotensin ii-induced cardiac remodeling by targeting STAT3. *Circulation Research*, *126*, 1007–1023. https://doi.org/10.1161/CIRCRESAHA.119.315861

Yuan, L. L., Green, A. S., Bertoli, S., Grimal, F., Mansat-De Mas, V., Dozier, C., Tamburini, J., Recher, C., Didier, C., & Manenti, S. (2014). Pim kinases phosphorylate Chk1 and regulate its functions in acute myeloid leukemia. *Leukemia*, *28*, 293–301. https://doi.org/10.1038/leu.2013.168

Zhao, M., Chow, A., Powers, J., Fajardo, G., & Bernstein, D. (2004). Microarray analysis of gene expression after transverse aortic constriction in mice. *Physiological Genomics*, *19*, 93–105.

Zhou, J., Wu, C., & Zhao, M. (2024). TAOK1-mediated regulation of the YAP/TEAD pathway as a potential therapeutic target in heart failure. *PLoS ONE*, *19*, e0308619.

Zhu, C., Yuan, T., & Krishnan, J. (2024). Targeting cardiomyocyte cell cycle regulation in heart failure. *Basic Research in Cardiology*, *119*, 349–369. https://doi.org/10.1007/s00395-024-01049-x

Zhu, L., Yu, Q., Gao, P., Liu, Q., Luo, X., Jiang, G., Ji, R., Yang, R., Ma, X., Xu, J., & Yuan, H. (2020). TAOK1 positively regulates TLR4-induced inflammatory responses by promoting ERK1/2 activation in macrophages. *Molecular Immunology*, *122*, 124–131.

SUPPORTING INFORMATION

Additional supporting information can be found online in the Supporting Information section at the end of this article.

How to cite this article: Xu, Z., Shen, Y., Luo, X., Wang, J., Zhou, Q., Han, X., Ren, J., Wang, L., & Liang, G. (2025). Angiotensin II-induced phosphorylation of CHK1 at serine-280 drives cardiac remodelling by direct phosphorylation of JAK1, thus activating JAK1-STAT signalling in murine cardiomyocytes. *British Journal of Pharmacology*, *182*(24), 6120–6135. https://doi.org/10.1111/bph.70180